Nonlocal Susceptibilities and Molecular Electric Quadrupole Moments of 3-Fluoropyridine and 2,6-Difluoropyridine, a Rotational Zeeman Effect Study

D. Hübner, M. Stolze, and D. H. Sutter

Abteilung Chemische Physik im Institut für Physikalische Chemie der Christian-Albrechts-Universität zu Kiel

Z. Naturforsch. **36a**, 332–346 (1981); received February 14, 1981

The rotational Zeeman effect spectra of 3-Fluoropyridine and 2,6-Difluoropyridine have been measured. The molecular g-values are $g_{aa} = -0.0917(5)$, $g_{bb} = -0.0476(5)$, $g_{cc} = +0.0194(5)$ for 3-Fluoropyridine and $g_{aa} = -0.0573(6)$, $g_{bb} = -0.0311(6)$, $g_{cc} = +0.0102(6)$ for 2,6-Difluoropyridine. The values for the magnetic susceptibility anisotropies in units of 10^{-6} erg/(G^2 mol) are $2X_{aa} + X_{bb} + X_{cc} = 53.3(8)$, $2X_{bb} - X_{cc} - X_{aa} = 60.5(7)$ for 3-Fluoropyridine and $2X_{aa} - X_{bb} - X_{cc} = 48.4(11)$, $2X_{bb} - X_{cc} - X_{aa} = 51.7(11)$ for 2,6-Difluoropyridine. Subtraction of the local atom contributions to the magnetic susceptibilities indicates that Fluorine quenching of the nonlocal out of plane contribution depends on the position of the substituent. Further, the data suggest a linear correlation between $X_{\perp}^{\text{nonlocal}}$ and the "CNDO/2-π-density alternation", which is used to predict susceptibility anisotropies of Fluorobenzenes and Fluoropyridines not yet measured.

The molecular quadrupole moments are calculated from the Zeeman data and compared with the experimental values obtained for various fluorosubstituted Pyridines and Benzenes. If the quadrupole moments perpendicular to the molecular plane are referred to the centers of the six membered rings and are plotted against the number of Fluoroine substituents, n_F, the plots closely follow a straight line with identical slopes for the Pyridine- and Benzenefamilies, but with different intercepts at $n_F = 0$. From the "$n_F = 0$ intercept" for the Fluorobenzenes we conclude that the Benzene quadrupole moment proposed earlier by Shoemaker and Flygare should probably be revised.

Introduction

The present investigation is part of a systematic study of substitution effects on the magnetic properties of five and six membered rings [1–8]. The ring currents presumed to flow in the cyclic π-electronic systems have been used for a long time as a criterion for aromaticity [9–15]. In NMR spectroscopy they manifest themselves in the deshielding of the protons of Benzene or in the large upfield shifts observed in the series of the Annulenes [16, 17, 18]. However caution is advisable in the inference of aromaticity on the basis of NMR data [18, 19]. For small rings the direct determination of the molecular susceptibility anisotropies from the molecular Zeeman effect is clearly to be preferred [20, 21, 22]. In such an experiment [23, 24] the splittings of the rotational transitions in the presence of a strong exterior magnetic field are measured with high precision in the microwave region. In part these splittings are caused by the anisotropy of the molecular susceptibility tensor. This anisotropy causes a field induced magnetic moment which is not exactly alligned to the exterior field and thus leads to a torque on the molecule which perturbs its overall rotation. With spherical symmetry of space reduced to axial symmetry around the field axis, the original M-degeneracy is lifted and the lines split. The direct observation of the susceptibility anisotropies is one advantage of our method. An other advantage is that the experiment is carried out in the gas phase. Thus a property of the free molecule is measured with no need for corrections of solvent effects etc. A second quantity of interest, which may be obtained from the molecular parameters determined in a rotational Zeeman effect study, is the tensor of the molecular electric quadrupole moment. Molecular quadrupole moments may be of importance for the close range orientational forces between molecules as for instance in liquids and in dimer formation. In a recent rotational energy transfer experiment on OCS, quadrupole type collisional selection rules were also found of comparable importance as dipole type selection rules [25, 26]. Although we believe that the structure of liquids is largely de-

Reprint request to Prof. Dr. D. H. Sutter, Institut für Physikalische Chemie der Universität Kiel, Abt. Chemische Physik, Olshausenstr. 40–60, D-2300 Kiel,

0340-4811 / 81 / 0400-0332 $ 01.00/0. — Please order a reprint rather than making your own copy.

termined by hard sphere repulsion and that the elongated attractive potential well of the Van der Waals forces of the rodlike OCS molecule is the main origin for the quadrupole type selection rules observed in rotational energy transfer, it is certainly desirable to have experimental values for the molecular quadrupole moments available at the present stage of our knowledge of intermolecular interactions.

Experimental Section

3-Fluoropyridine (b.p. 105 °C at 752 Torr [27] and 2,6-Difluoropyridine (b.p. 123 °C at 743 Torr [28] both colourless liquids, were purchased from Pfaltz and Bauer and PCR Research Chemicals Inc. respectively. After a vacuum distillation they were used without further purification. The zero field microwave spectra of both compounds have been previously assigned [29—32]. However, in order to minimize the effect of experimental uncertainties in the ^{14}N quadrupole coupling constants and zero field frequencies, we remeasured the zero field hyperfine patterns of several low J transitions for both molecules. A standard microwave spectrometer with 33 kHz square wave Stark effect modulation and phase stabilized BWOs as radiation sources was used for these measurements [33, 34]. For both mol-

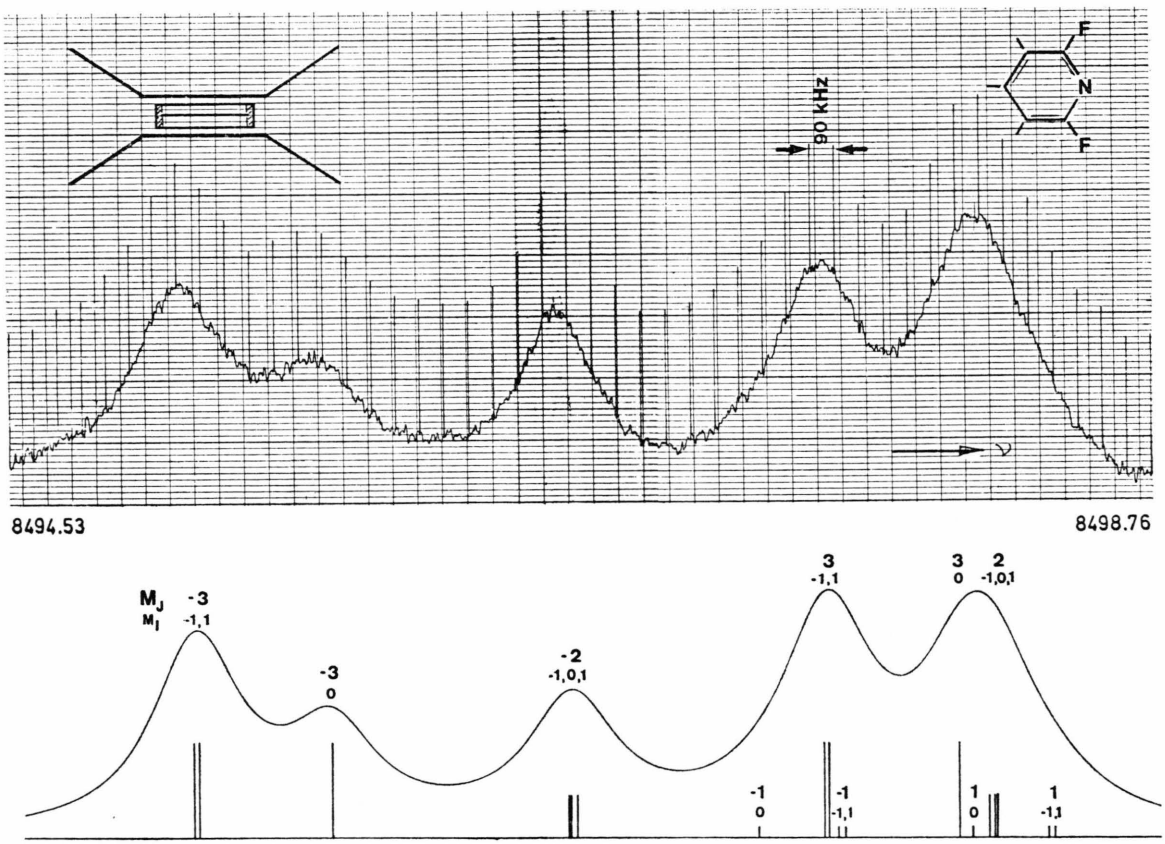

Fig. 1. Typical recorder traces of Zeeman-hyperfine patterns of the Fluoropyridines. Fig. 1a shows a recording of the $3_{13} \rightarrow 3_{22}$ transition in 2,6-Difluoropyridine observed at a field of 22.94 kG. The recording covers the frequency range from 8494.53 MHz (left) to 8498.76 MHz (right). The lower trace shows a computer simulation of this transition with satellite frequencies and relative intensities calculated from the rotational constants and ^{14}N-quadrupole coupling constants listed in Table 3, from the g-values and susceptibility anisotropies listed in Table 4 and under the assumption of Lorentzian line shapes with halfintensity halfwidths of 250 kHz for each individual satellite. The insert shows the orientation of the waveguide cross section between the tapered poles of the electromagnet. With the electric field vector of the incident microwave radiation parallel to the exterior field, which very effectively uncouples ^{14}N-spin and overall rotation, $\Delta M_J = 0$ and $\Delta M_I = 0$ selection rules apply [24]. The bar spectrum shows the positions and relative intensities of the individual satellites with their characterizing M_J and M_I values given on top.

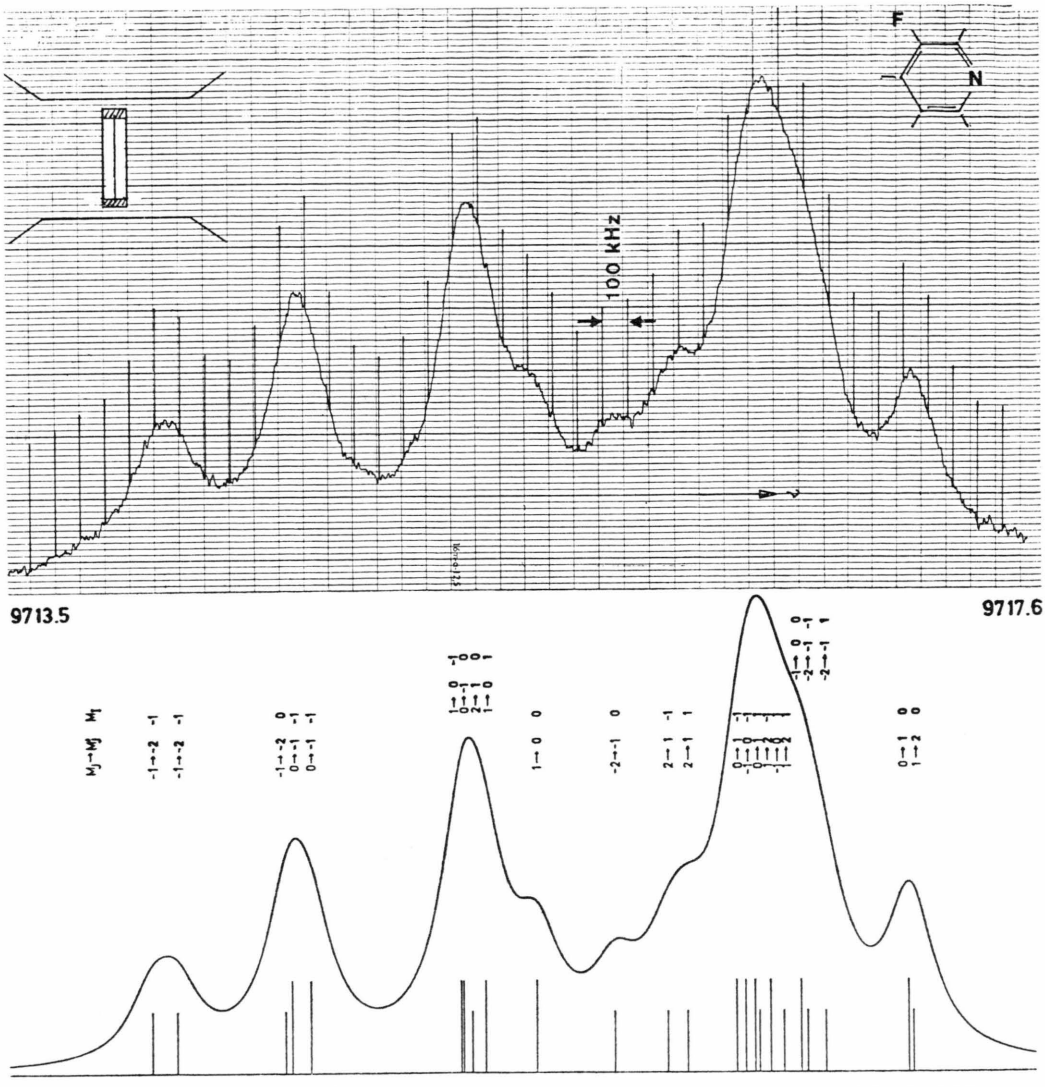

In Fig. 1b a similar recording and computer simulation is shown for the $2_{11} \rightarrow 2_{20}$ transition in 3-Fluoropyridine, observed at a field of 17.09 kG under $\Delta M_J = \pm 1$, $\Delta M_I = 0$ selection rules (see insert). The frequency range is 9713.5 MHz (left) and 9717.6 MHz (right).

ecules collisional line broadening is rather strong as a result of the fairly large electric dipole moments ($|\mu_a| = 0.39$ D, $|\mu_b| = 2.05$ D for 3-Fluoropyridine [29] and $|\mu_b| = 3.82$ D for 2,6-Difluoropyridine [32]. Even at pressures as low as 1 to 10 m Torr in oversized waveguide absorption cells (inner cross section: 1×5 cm) linewidths were on the order of $\Delta\nu_{1/2} = 150$ kHz (half height halfwidth). With signal to noise ratios, S/N, typically around 30 (see Fig. 1), the spectroscopic rule of thumb suggests an upper limit to the experimental uncertainty, $\delta\nu_0$, in our frequency determinations,

$$\delta\nu_0 = \sqrt{N/S} \cdot \Delta\nu_{1/2},$$

which is on the order of 25 to 30 kHz.

The observed zero field frequencies are listed in Table 1. The data were analysed within the standard rigid rotor approximation. For the calculation of the frequencies a computer program was written in which the Hamiltonian matrix is set up in the coupled basis $|J, K, I, F, M_F\rangle$ [35]. The matrix factorizes into blocks corresponding to the different

Table 1. Observed and calculated rotational transition frequencies in 3-Fluoropyridine and 2,6-Difluoropyridine. The calculated frequencies follow from the rotational constants and ^{14}N nuclear quadrupole coupling constants listed in Table 2 and Table 3 within the rigid rotor model. The Hamiltonian matrix was set up in the coupled basis $|J, K, I, F, M_F\rangle$ [35] and diagonalized numerically.

3-Fluoropyridine						2,6-Difluoropyridine				
Rotational	Transition					Rotational	Transition			
$J_{K_-K_+} \leftarrow J'_{K_-'K_+'}$	$F \leftarrow F'$		ν_{obs} MHz	ν_{calc} MHz	$\Delta\nu_{obs-calc}$ MHz	$J_{K_-K_+} \leftarrow J'_{K_-'K_+'}$	$F \leftarrow F'$		ν_{obs} MHz	ν_{calc} MHz	$\Delta\nu_{obs-calc}$ MHz
$1_{11} \leftarrow 0_{00}$	2	1	7 645.54	7 645.54	0.00						
$1_{11} \leftarrow 0_{00}$	1	1	7 644.52	7 644.51	0.01						
$1_{11} \leftarrow 0_{00}$	0	1	7 647.08	7 647.09	− 0.01						
$2_{20} \leftarrow 2_{11}$	3	3	9 716.06	9 716.04	0.02	$3_{22} \leftarrow 3_{13}$	3	3	8 497.82	8 497.83	− 0.01
$2_{20} \leftarrow 2_{11}$	2	2	9 715.21	9 715.20	0.01	$3_{31} \leftarrow 3_{22}$	4	4	10 896.08	10 896.07	0.01
$2_{20} \leftarrow 2_{11}$	1	1	9 716.52	9 716.51	0.01	$3_{31} \leftarrow 3_{22}$	3	3	10 895.38	10 895.36	0.02
$2_{21} \leftarrow 2_{12}$	3	3	12 041.81	12 041.82	− 0.01	$4_{23} \leftarrow 4_{14}$	4	4	9 904.33	9 904.31	0.02
$2_{21} \leftarrow 2_{12}$	2	2	12 042.92	12 042.91	0.01	$4_{40} \leftarrow 4_{31}$	4	4	14 807.20	14 807.21	− 0.01
$2_{21} \leftarrow 2_{12}$	1	1	12 041.22	12 041.23	− 0.01	$4_{40} \leftarrow 4_{31}$	5	5	14 808.16	14 808.16	0.00
$3_{21} \leftarrow 3_{12}$	3	3	9 110.91	9 110.94	− 0.03	$5_{14} \leftarrow 5_{05}$	6	6	9 331.33	9 331.36	− 0.03
$4_{23} \leftarrow 4_{14}$	5	5	15 128.98	15 128.99	− 0.01	$5_{14} \leftarrow 5_{05}$	5	5	9 333.06	9 333.07	− 0.01
$4_{23} \leftarrow 4_{14}$	4	4	15 130.30	15 130.27	0.03	$5_{14} \leftarrow 5_{05}$	4	4	9 331.03	9 331.01	0.02
$4_{23} \leftarrow 4_{14}$	3	3	15 128.69	15 128.66	0.03	$5_{33} \leftarrow 5_{24}$	6	6	11 863.90	11 863.88	0.02
$4_{13} \leftarrow 4_{04}$	5	5	9 163.78	9 163.79	− 0.01	$5_{42} \leftarrow 5_{33}$	5	5	14 938.61	14 938.64	− 0.03
$4_{13} \leftarrow 4_{04}$	4	4	9 165.69	9 165.67	0.02	$2_{12} \leftarrow 1_{01}$	2	1	7 536.40	7 536.40	0.00
$4_{13} \leftarrow 4_{04}$	3	3	9 163.30	9 163.31	− 0.01	$2_{12} \leftarrow 1_{01}$	3	2	7 537.68	7 537.68	0.00
						$2_{12} \leftarrow 1_{01}$	2	2	7 536.97	7 536.97	0.00

F values (F = overall angular momentum quantum number corresponding to rotational angular momentum (J) plus ^{14}N spin (I)). In each such block J runs from $F - I$ to $F + I$ in steps of one. The eigenvalues were obtained by numerical diagonalization. Our final rotational constants and quadrupole coupling constants resulting from a least squares fit [36] to the observed frequencies are listed in Table 2 (3-Fluoropyridine) and Table 3 (2,6-Difluoropyridine).

The microwave spectrometer and high-field electromagnet used in the Zeeman study have been described previously [37]. For the analysis of the splittings the Hamiltonian matrix, now including matrix elements arising from the ^{14}N nuclear Zeeman effect and the first and second order rotational Zeeman effect was set up in the uncoupled basis $|I, M_I, J, K, M_J\rangle$. Spin rotation interaction and anisotropies in the ^{14}N-shielding tensor were neglected. Also matrix elements connecting different rotational states were neglected throughout. Except for the $2_{2\,1}$ and $3_{1\,3}$ states in 3-Fluoropyridine which show an accidental close degeneracy and therefore were not included in the analysis of data, this approximation is excellent for the given experimental accuracy. The explicit expressions for the nonzero matrix elements used in the work reported here have been given previously [38].

With the obtainable resolution (see above) overlapping of Zeeman-hyperfine satellites was frequent. In such cases the observed peak frequencies were assumed to represent the intensity weighted means of the corresponding satellite frequencies. As an example in Fig. 1 a ($3_{13} \rightarrow 3_{22}$ transition in 2,6-Difluoropyridine) the peak frequency of the third satellite from left was assumed to be the intensity weighted means of three satellites denoted by their M_J, M_I numbers, namely $-2, -1$ ($n = 1$), $-2,0$ ($n = 2$) and $-2,1$ ($n = 3$) and accordingly its shift with respect to the hypothetical rigid rotor zero field frequency, $\Delta\nu_{Peak}$, was assumed to equal the intensity weighted means of the three corresponding linear Equations of type

$$\Delta\nu_n^{exp} = \Delta\nu_n^{calc} + \sum_{\gamma=a,b,c}\left(\frac{\partial\Delta\nu_n}{\partial g_{\gamma\gamma}}\right)\Delta g_{\gamma\gamma} + \left(\frac{\partial\Delta\nu_n}{\partial X_1}\right)\Delta X_1 + \left(\frac{\partial\Delta\nu_n}{\partial X_2}\right)\Delta X_2$$

used in the least squares procedure to determine the corrections Δg_{aa} etc. to the initial g-values and

Table 2. Rigid rotor rotational constants and ^{14}N nuclear quadrupole coupling constants for 3-Fluoropyridine. Also given for comparison are the values determined earlier by Sharma and Doraiswamy [30]. Due to the accidental close degeneracy of the 2_{21} and 3_{13} rotational levels, which is associated with quadrupole coupling matrix elements connecting these levels, X^N_{ab} can be determined from the "irregularities" in the hyperfine patterns of the corresponding transitions. Although only $|X^N_{ab}|$ is determined from the experiment, the sign is clearly negative. [Rotation of the Pyridine ^{14}N quadrupole coupling tensor (see G. O. Sørensen, J. Mol. Spectry **22**, 325 (1967).) by 60° (compare Fig. 2b) would lead to $X^N_{ab} = -2.73$ MHz]. The numbers in brackets give the single standard deviations in units of the least significant figure of the preceeding value.

		This work	Sharma et al.
Rotational constants	A/MHz	5829.703(9)	5829.661(20)
$A = h/(8\pi^2 I_{aa})$	B/MHz	2637.499(9)	2637.465(7)
$I_{aa} = \sum_n^{\text{atoms}} m_n(b_n^2 + c_n^2)$	C/MHz	1815.669(9)	1815.648(8)
m_n = atomic mass of n-th atom			
b_n, c_n = coordinates of n-th atom			
^{14}N quadrupole coupling constants	X^N_{aa}/MHz	− 0.03(4)	0.06(3)
$X^N_{aa} = eQ\left\langle\left\vert\frac{\partial^2 V}{\partial a^2}\right\vert\right\rangle/h$ etc.	X^N_{bb}/MHz	− 3.43(7)	− 3.52(8)
e = proton charge	X^N_{cc}/MHz	3.46(7)	3.46(8)
Q = ^{14}N nuclear quadrupole moment	X^N_{ab}/MHz	− 2.33(23)	—
$\left\langle\left\vert\frac{\partial^2 V}{\partial a^2}\right\vert\right\rangle$ = electronic ground state expectation value of second derivative of intramolecular Coulomb potential at position of ^{14}N nucleus caused by the extranuclear charge distribution.			

susceptibility anisotropies $X_1 = 2X_{aa} - X_{bb} - X_{cc}$ and $X_2 = 2X_{bb} - X_{cc} - X_{aa}$. The molecular parameters which can be derived from the Zeeman splittings are listed in Table 4. The bulk susceptibilites entering into this analysis were estimated from Pascals rules using the experimental bulk susceptibility for Pyridine

$$(X_{\text{Pyridine}} = -49.2 \cdot 10^{-6}\,\text{erg}/(\text{G}^2\,\text{mol})) \quad [39]$$

together with Pascals constants for Fluorine

$$(C_{\text{F}} = -6.3 \cdot 10^{-6}\,\text{erg}/(\text{G}^2\,\text{mol}))$$

Table 3. Rigid rotor rotational constants and ^{14}N nuclear quadrupole coupling constants for 2,6-Difluoropyridine resulting from a least squares fit to the frequencies listed in Table 1. Also given for comparison are the corresponding values published earlier by Doraiswamy and Sharma [31] and by Stiefvater [32].

	This work	Doraiswamy et al.	Stiefvater
A/MHz	3747.680(4)	3747.681(7)	3747.701(8)
B/MHz	1905.825(4)	1905.817(3)	1905.832(4)
C/MHz	1263.249(4)	1263.246(3)	1263.253(4)
X^N_{aa}/MHz	1.91(4)	1.91(14)	1.82(5)
X^N_{bb}/MHz	− 4.12(6)	− 4.24(4)	− 4.16(2)
X^N_{cc}/MHz	2.21(6)	2.33(10)	2.34(5)

and for Hydrogen

$$(C_{\text{H}} = -2.9 \cdot 10^{-6}\,\text{erg}/(\text{G}^2\,\text{mol})), \quad [40].$$

The resulting bulk susceptibilities were assumed to be accurate only within 10%, to account for the experimental uncertainties in the Pyridine value, for the approximative nature of Pascals rules, and for possible differences between gas phase susceptibilities and liquid phase values. The geometries for the nuclear frames which also enter into the analysis of the data were taken from the literature [30, 31]. They correspond to partial r_0-structures and are given in Figure 2.

Discussion

The magnetic criterion for aromaticity from the molecular Zeeman effect has been discussed in detail by Schmalz et al. [20]. Their method involves the determination of the "nonlocal" contribution to the out-of-plane magnetic susceptibility by subtraction of the contribution from "local" atom values. The latter are empirically determined from a least squares fit to the susceptibilities of a large set of open chain molecules whose values are assumed to be entirely local in nature. The method is described also in [41].

Table 4. Diagonal elements of the molecular g-tensor, anisotropies of the diagonal elements of the magnetic susceptibility tensor and molecular parameters which can be derived from these Zeeman data, from the bulk susceptibility and from the structure of the nuclear frame (see Figure 2). In principle two sets of g-values which differ only in sign are compatible with the observed Zeeman patterns [24, 25]. However the sets with opposite signs may be discarded since they would lead to unreasonably large quadrupole moments and negative values for the electronic ground state expectation values

$$\langle 0| \sum_{\varepsilon}^{\text{electrons}} c_\varepsilon^2 |0\rangle.$$

		3-Fluoro pyridin	2,6-Difluoro-pyridin
Molecular g-values	g_{aa}	− 0.0917 (5)	− 0.0573 (6)
	g_{bb}	− 0.0476 (5)	− 0.0311 (6)
	g_{cc}	0.0194 (5)	0.0102 (6)
Molar magnetic susceptibility anisotropies	$\frac{N_L(2\chi_{aa} - \chi_{bb} - \chi_{cc})}{[10^{-6}\,\text{erg}/(\text{G}^2\,\text{mole})]}$	53.3 (8)	48.4 (11)
	$\frac{N_L(2\chi_{bb} - \chi_{cc} - \chi_{aa})}{[10^{-6}\,\text{erg}/(\text{G}^2\,\text{mole})]}$	60.5 (7)	51.7 (11)
	χ_{bulk}	−52.6 (50)	−56.0 (50)
Molecular quadrupole moments in units of 10^{-26} esu cm^2	Q_{aa}	− 1.2 (12)	− 0.4 (20)
$Q_{aa} = \frac{\lvert e\rvert}{2}\left\{\sum_n^{\text{nuclei}} Z_n(2a_n^2 - b_n^3 - c_n^2) - \langle 0\rvert \sum_\varepsilon^{\text{electrons}} (2a_\varepsilon^2 - b_\varepsilon^2 - c_\varepsilon^2)\lvert 0\rangle\right\}$	Q_{bb}	3.2 (13)	1.5 (22)
$= -\frac{h\lvert e\rvert}{16\pi^2 m_p}\left\{\frac{2g_{aa}}{A} - \frac{g_{bb}}{B} - \frac{g_{cc}}{C}\right\} - \frac{2mc^2}{\lvert e\rvert}(2\chi_{aa} - \chi_{bb} - \chi_{cc})$	Q_{cc}	− 2.0 (18)	− 1.0 (30)
Magnetic susceptibilities in units of 10^{-6} erg/(G^2 mole)	χ_{aa}	−34.8 (56)	−39.9 (54)
	χ_{bb}	−32.4 (55)	−38.8 (54)
	χ_{cc}	−90.5 (58)	−89.3 (58)
Second moments of the nuclear charge distribution calculated from the geometry of the nuclear frame given in Å^2	$\sum_n Z_n c_n^2$	99.7 (1)	132.2 (1)
	$\sum_n Z_n b_n^2$	74.1 (1)	73.2 (1)
	$\sum_n Z_n a_n^2$	0.0 (0)	0.0 (0)
Second moments of the electronic charge distribution in Å^2	$\langle 0\rvert \sum_\varepsilon a_\varepsilon^2\lvert 0\rangle$	108.0 (24)	140.9 (2σ)
$\left\langle 0\rvert \sum_\varepsilon^{\text{electrons}} a_\varepsilon^2\lvert 0\right\rangle = -\frac{2mc^2}{e^2}(\chi_{bb} + \chi_{cc} - \chi_{aa})$	$\langle 0\rvert \sum_\varepsilon b_\varepsilon^2\lvert 0\rangle$	81.9 (24)	81.6 (24)
$-\frac{h}{16\pi^2 m_p}\left(\frac{g_{bb}}{B} + \frac{g_{cc}}{C} - \frac{g_{aa}}{A}\right) - \sum_n^{\text{nuclei}} Z_n a_n^2$	$\langle 0\rvert \sum_\varepsilon c_\varepsilon^2\lvert 0\rangle$	8.4 (24)	8.7 (24)

Since the work of Schmalz et al. the set of open chain molecules available for the determination of the local atom susceptibilities has increased considerably, which has lead to improved local values [42, 43]. In Table 5 we list those local susceptibilities which are of relevance here.

In Table 6 we compare experimental and nonlocal susceptibilities of various aromatic molecules. Isoprene at the top of the list is included as an example of an open chain molecule in which quite generally *all* components of the susceptibility tensor are resonable well reproduced by the local model. For aromatic molecules this is true only for the in-plane components.

We will now first present a qualitative discussion of the difference observed for the nonlocal out-of-plane susceptibilities of 2-Fluoropyridine [3] and of 3-Fluoropyridine. In the subsequent section we will demonstrate that a linear relation appears to hold between the nonlocal out-of-plane susceptibility and the "π-density alternation" calculated from the semiempirical CNDO/2 program [45]. This linear relation may then be used to predict the susceptibilities of the Fluorobenzenes and Fluoropyridines not yet measured so far.

We now enter the discussion of the difference in the nonlocal out of plane susceptibilities of 2- and 3-Fluoropyridine. They are not measured directly, but with two assumptions inherent to the model of local atom susceptibilities it follows that their difference is equal to the difference of the experimentally determined $X_{cc} - (X_{aa} + X_{bb})/2$ values of the

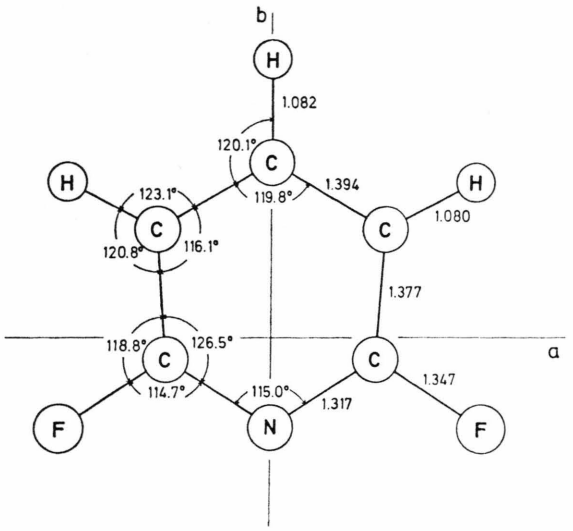

(a)

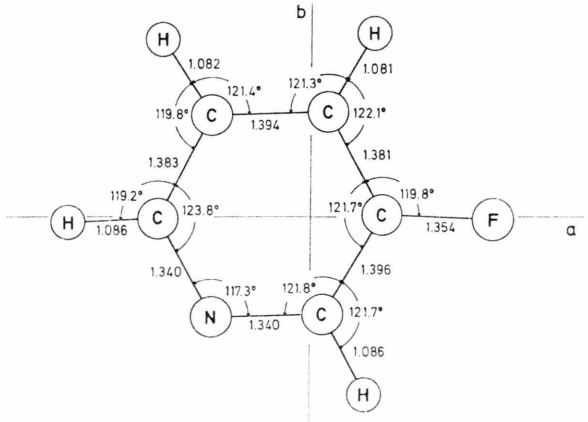

(b)

Fig. 2. Structures for 2,6-Difluoropyridine (a) [31] and 3-Fluoropyridine (b) [30] used for the analysis of the rotational Zeeman effect data. Also indicated is the principal inertia axes system originating at the molecular center of mass.

Table 5. Increments of local atom magnetic susceptibilities [24, 42, 43] used for the calculations of X^{local}. They are given in units of 10^{-6} erg/(G² mol). The Nitrogen values are based on only one molecule, Nitrosylfluoride (FNO) [44].

	Atom	$(X_{xx}+X_{yy})/2$	X_{zz}
y	H—	− 1.70	− 2.11
▲	>C=	− 3.54	− 7.11
└▶	S<	− 1.70	− 14.8
	N≪	0	− 4.0
x	F—	− 7.6	− 5.6

Table 6. Comparison of experimental susceptibilities and susceptibilities calculated within the local model from atomic increments. The values are given in units of 10^{-6} erg/(Gauss² mol). In all cases the *c*-axis is perpendicular to the heavy atom plane.

	Experimental susceptibilities $X_{\parallel}=(X_{aa}+X_{bb})/2$ $X_{\perp}=X_{cc}$	Nonlocal susceptibilities $X_{\parallel}=(X_{aa}+X_{bb})/2$ $X_{\perp}=X_{cc}$
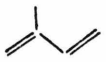	− 35.7[a] − 52.8	1.6 − 0.3
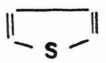	− 40.7[b] − 90.8	− 2.8 − 39.1
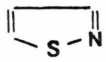	− 33.6[c] − 84.6	− 1.0 − 38.1
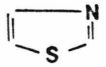	− 32.8[c] − 86.1	− 0.2 − 39.6
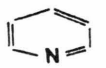	− 29.4[d] − 86.8	− 3.2 − 36.7
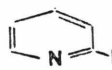	− 35.2[e] − 87.4	− 3.1 − 33.9
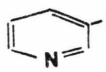	− 33.6[f] − 90.5	− 2.0 − 36.1
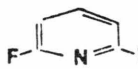	− 39.4[f] − 89.3	− 1.8 − 31.5

[a] T. G. Schmalz, C. L. Norris, and W. H. Flygare, J. Amer. Chem. Soc. **95**, 7961 (1973).
[b] D. H. Sutter and W. H. Flygare, J. Amer. Chem. Soc. **91**, 4063 (1969).
[c] J. Wiese and D. H. Sutter, Z. Naturforsch. **35a**, 712 (1980).
[d] J. H. S. Wang and W. H. Flygare, J. Chem. Phys. **52**, 5636 (1970).
[e] D. H. Sutter, Z. Naturforsch. **26a**, 1644 (1971).
[f] this work.

two molecules (see Table 4 and Ref. [3]). The two assumptions are

i) The local atom susceptibilities are independent of the neighbouring atoms [46]. (Within this assumption both molecules have identical local susceptibilities X_{cc}^{local} and $(X_{aa}^{\text{local}}+X_{bb}^{\text{local}})/2$).

ii) Nonlocal (π-electronic ring current) contributions are present only in the out of plane susceptibilities, i.e. $X_{aa}=X_{aa}^{\text{local}}$, $X_{bb}=X_{bb}^{\text{local}}$, but $X_{cc}=X_{cc}^{\text{local}}+X_{cc}^{\text{nonlocal}}$.

Within this model we conclude from the experimental values listed in Table 4 and

$$X_{cc} - (X_{aa} + X_{bb})/2 = -52.1 \cdot 10^{-6}\ \mathrm{erg/(G^2\,mol)}$$

for 2-Fluoropyridine that the absolute value of $X_{cc}^{\mathrm{nonlocal}}$ is 4.8 mu smaller in 2-Fluoropyridine than is its value in 3-Fluoropyridine, with an experimental uncertainty of ± 1.1 mu. (In this case the difference of the $X_{cc}^{\mathrm{nonlocal}}$-values can be determined with higher accuracy than the diagonal elements of the X-tensor themselves whose precision suffers from the uncertainty in the bulk value). Thus, with $X_{cc}^{\mathrm{nonlocal}}$-values on the order of -34 mu (see Table 6), the nonlocal out of plane susceptibility of 2-Fluoropyridine is quenched about 14% if compared to its value in 3-Fluoropyridine.

Since the π-electrons are probably more localized in 2-Fluoropyridine than in 3-Fluoropyridine (see Fig. 3 and Table 7), this result might have been expected intuitively. It is however also possible to rationalize it from the theoretical expression for the out of plane susceptibility which is given in Equation (1).

$$X_{cc} = -\frac{e^2}{4mc^2}\left\langle 0\left|\sum_{\varepsilon}^{\text{electrons}}(a_\varepsilon^2 + b_\varepsilon^2)\right|0\right\rangle - \frac{e^2}{2m^2c^2}\sum_{n}^{\text{ex. states}}\frac{|\langle n|\hat{L}_c|0\rangle|^2}{E_0 - E_n} = X_{cc}^{\mathrm{diamagnetic}} + X_{cc}^{\mathrm{paramagnetic}}. \quad (1)$$

In Eq. (1) the symbols have the following meanings:
e = electron charge, m = electron mass, c = velocity of light, a_ε, b_ε = a- and b-coordinates of the ε-th electron,

$$\hat{L}_c = \frac{\hbar}{i}\sum_{\varepsilon}\left(a_\varepsilon\frac{\partial}{\partial b_\varepsilon} - b_\varepsilon\frac{\partial}{\partial a_\varepsilon}\right)$$

= operator corresponding to the c-component of the electronic angular momentum with respect to the molecular axes system (see for instance Ref. [24], Chap. IV).

E_n = n-th eigenvalue of the electronic Schrödinger equation (infinite nuclear mass approximation).

$|0\rangle$, $|n\rangle$ = electronic ground state and n-th excited state wave functions respectively.

Consideration of "localization" is equivalent to a discussion of Eq. (1) in terms of matrixelements. Localization of π-electrons at certain ring atoms has little effect on $X_{cc}^{\mathrm{diamagnetic}}$. (The radiusvectors to the ring atoms have essentially the same lengths.) We

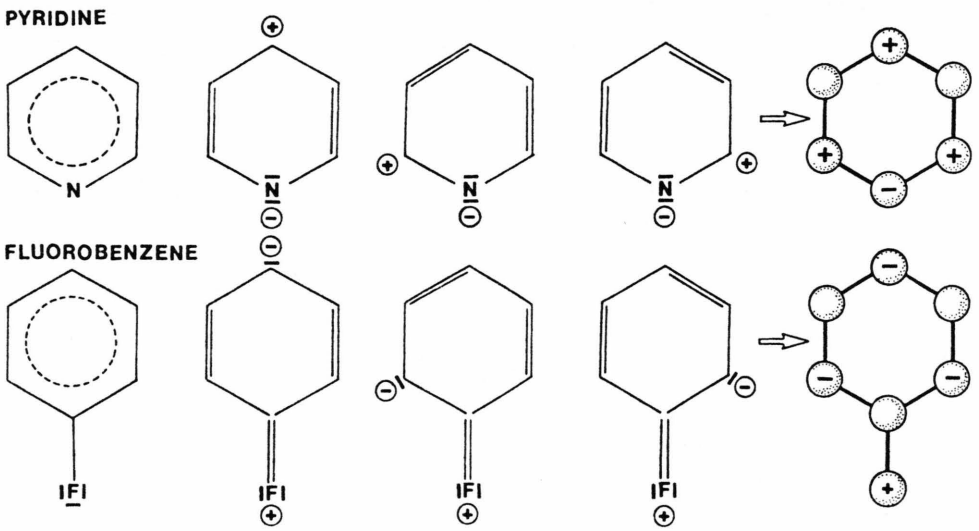

Fig. 3. In a simple picture "resonance" between the dominant valence structures (left) and valence structures which would correspond to localized double bonds leads to slightly bumpy π-electron distributions (right) for Pyridine and Fluorobenzene. Superposition of these to form the π-system of 2-Fluoropyridine and 3-Fluoropyridine should lead to an increased bumpiness (localization) in 2-Fluoropyridine and to a smoother, more delocalized, π-density in 3-Fluoropyridine. Corresponding to the higher localization of the π-electrons in 2-Fluoropyridine one would expect a reduced nonlocal (ring current) contribution to the out of plane component of the susceptibility tensor and this is actually observed.

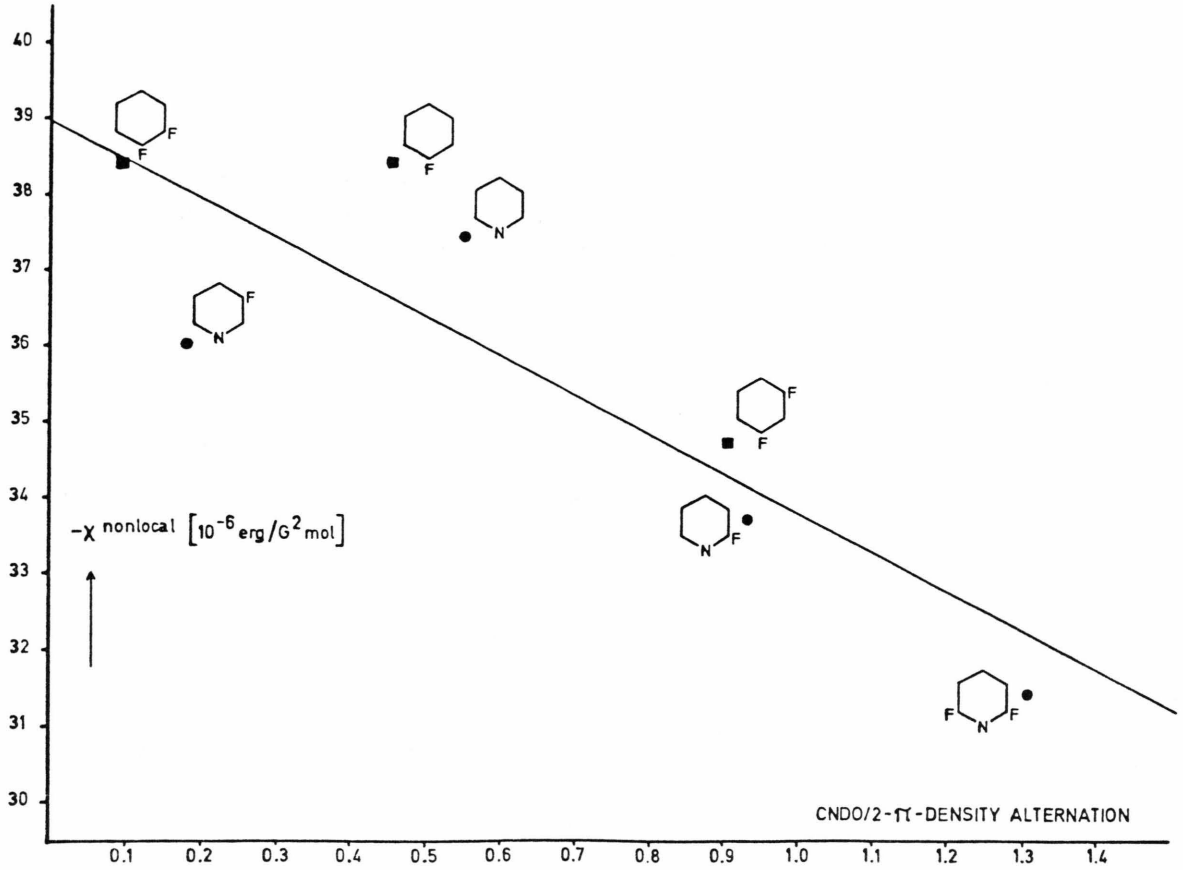

Fig. 4. A plot of the nonlocal contribution to the susceptibility component perpendicular to the molecular plane versus the calculated CNDO/2-π-density alternation defined in the text suggests a linear relationship, which may be used to predict $X_{\perp}^{\mathrm{nl}}$ from calculated CNDO/2 values for Fluorobenzenes and Fluoropyridines not measured so far. Assuming that only the out-of-plane component of X contains a nonlocal contribution, Table 5 may then be used to predict the complete susceptibility tensors for these molecules.

therefore have to concentrate on $X_{cc}^{\mathrm{paramagnetic}}$ which partly compensates $X_{cc}^{\mathrm{diamagnetic}}$. Since $\hat{L}_c|0\rangle$ is zero for wave functions with cylindrical symmetry around the c-axis [47], all matrixelements in the perturbation sum would vanish for such wave functions and there would be no paramagnetic compensation for $X_{cc}^{\mathrm{diamagnetic}}$ in molecules with completely delocalized wave functions. A certain bumpiness of the ground state wave function is therefore essential for the presence of a paramagnetic contribution. This prompted us to look for a correlation between the nonlocal out of plane susceptibility and the "π-electron-density alternation" along the ring. The latter was calculated within the CNDO/2 approximation [45]. As "π-density alternation" we have defined the sum of the absolute values of the p_z-population differences of the neighbouring ring atoms:

$$\text{"}\pi\text{-density alternation"} = \sum_{n=1}^{\text{ring atoms}} |P_{p_z p_z}^{(n)} - P_{p_z p_z}^{(n-1)}|$$

with $n =$ number of the ring atoms and with the additional convention

$$P_{p_z p_z}^{(0)} = P_{p_z p_z}^{(6)}.$$

In Fig. 4 we present a plot of $X_{cc}^{\mathrm{nonlocal}}$ values versus the corresponding "π-density alternations" defined above. The CNDO/2-populations used in this plot are listed in Tables 7 and 8.

The susceptibilities are listed in Table 9. Keeping in mind that the uncertainties in the $X_{cc}^{\mathrm{nonlocal}}$-values are typically on the order of 2 mu, Fig. 4 suggests

Table 7. CNDO/2 p_z-populations for the ring atoms in Pyridine and several Fluoropyridines. We used POPLE's CNDO/2 program with its original parametrization [45]. The p_z-populations at the i-th ring atom are defined as

$$P^{(i)}_{p_z p_z} = 2 \sum_{n}^{\text{occ. orb.}} |c^{(i)}_{n p_z}|^2,$$

where $c^{(i)}_{n p_z}$ is the coefficient of the corresponding p_z-orbital in the n-th molecular orbital and where the sum runs over all occupied orbitals.

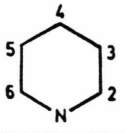	1	2	3	4	5	6
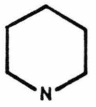	1.066	0.957	1.036	0.949	1.036	0.957
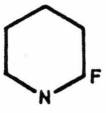	1.116	0.927	1.082	0.928	1.060	0.937
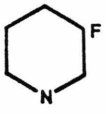	1.046	1.001	1.005	0.994	1.015	0.981
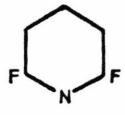	1.166	0.908	1.106	0.908	1.106	0.908
	1.094	0.937	1.080	0.922	1.080	0.937
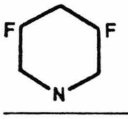	1.025	1.025	0.985	1.041	0.985	1.025

Table 8. CNDO/2 p_z-populations for the ring atoms of several Fluorobenzene (see also Table 7). They are used to calculate the "CNDO/2-π-density alternation" defined in the text. See also Figure 4.

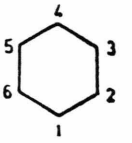	1	2	3	4	5	6
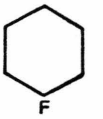	0.963	1.055	0.976	1.031	0.976	1.055
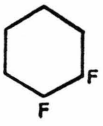	1.014	1.014	1.031	1.006	1.006	1.031
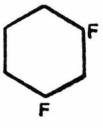	0.939	1.111	0.939	1.086	0.952	1.086
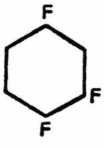	1.044	0.990	1.087	0.967	1.061	1.006
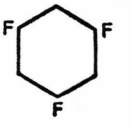	0.917	1.142	0.917	1.142	0.917	1.142
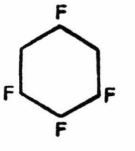	1.099	0.967	1.118	0.943	1.118	0.967
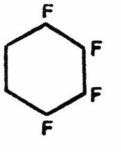	1.020	1.044	1.044	1.020	1.036	1.036
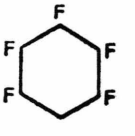	1.093	0.995	1.075	1.021	1.075	0.995
	1.050	1.050	1.050	1.050	1.050	1.050

Table 9. Experimental susceptibilities (left) and susceptibilities predicted from the local model and from the correlation between the nonlocal contribution to the out of plane susceptibility and the "CNDO/2-π-density alternation" shown in Fig. 4 (right). The local values are calculated from Table 5. All values are in units of 10^{-6} erg/(G^2 mol). For the seven molecules listed at right no experimental values are available at present. Their susceptibilities are predicted under the assumption that only the out of plane component contains a nonlocal contribution. The latter is predicted from the calculated "CNDO/2-π-density alternation" (see Tables 7 and 8) according to Figure 4. We expect our predictions to be accurate within $2 \cdot 10^{-6}$ erg/(G^2 mol). For the references see Table 6 and the list at the end of this contribution. The Pyridine susceptibilities given here correspond to meanvalues calculated from the experimental data of Pyridine-N^{15}, Pyridine-N^{14} and of Paradeuteropyridine-N^{14} and thus differ slightly from the values given in Table 6.

	$X_{\parallel}^{\text{experimental}}$ $X_{\parallel}^{\text{local}}$	$X_{\perp}^{\text{experimental}}$ $X_{\perp}^{\text{local}}$		$X_{\parallel}^{\text{predicted}}$ $(= X_{\parallel}^{\text{local}})$	$X_{\perp}^{\text{predicted}}$ $X_{\perp}^{\text{local}}$
	− 35.9 − 37	− 97.2 − 59		− 49*	− 98* − 66
	− 45.9 − 43	− 97.0 − 62	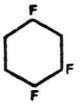	− 49*	− 103* − 66
	− 46.4 − 43	− 100.7 − 62	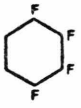	− 55*	− 108* − 69
	− 30.1 − 26	− 87.5 − 50		− 61*	− 110* − 71
	− 35.2 − 32	− 87.4 − 54	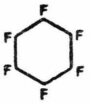	− 67*	− 115* − 76
	− 33.6 − 32	− 90.5 − 54		− 32*	− 88* − 54
	− 39.4 − 38	− 89.3 − 57		− 38*	− 95* − 57

a linear relationship between X_{cc}^{nonlocal} and the "CNDO/2-π-density alternation" defined above. We have used this linear relationship to predict susceptibilities of Fluorobenzenes and Fluoropyridines which have not yet been investigated by the rotational Zeeman effect technique. To this end we used the calculated $P_{p_x p_z}^{(n)}$-values to interpolate the nonlocal contribution to X_{cc} from the least squares straight line in Figure 4. The susceptibilities were then calculated under the assumption that only X_{cc} contains a nonlocal contribution. The results are marked by an asterisk in Table 9. We note that susceptibility anisotropy obtained that way for Benzene is considerably higher than the value of − 53.9 $\pm$ 2.5 mu deduced by Buckingham and coworkers from Cotton-Mouton effect experiments [48]. We believe that our arguments concerning this difference [6] still hold.

We now turn to the discussion of the out of plane components of the molecular electric quadrupole moments, $Q_{\perp} = Q_{cc} = Q_{zz}$. Figure 5, together with the theoretical expression for the quadrupole moment (see Eq. (2)) suggests that a linear relation between $Q_{\perp}$ and the number of Fluorine substituents might hold to a good approximation if all $Q_{\perp}$'s are referred to the center of the six membered ring.

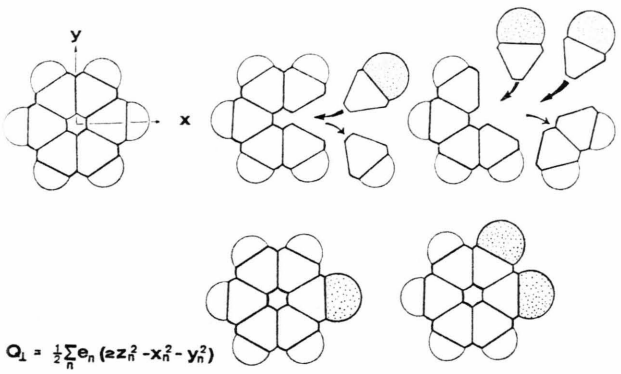

Fig. 5. Within a simplified model one might expect the out of plane component of the molecular electric quadrupole moment to depend linearity on the number of Fluorine substituents, n_F, provided it is referred to the center of the ring. In that case shifts of electron charge along the perimeter of the ring, such as were discussed in the context of the nonlocal out of plane susceptibility, should have very little effect on $Q_\perp$ since they leave $r_n^2 = x_n^2 + y_n^2$ essentially unchanged.

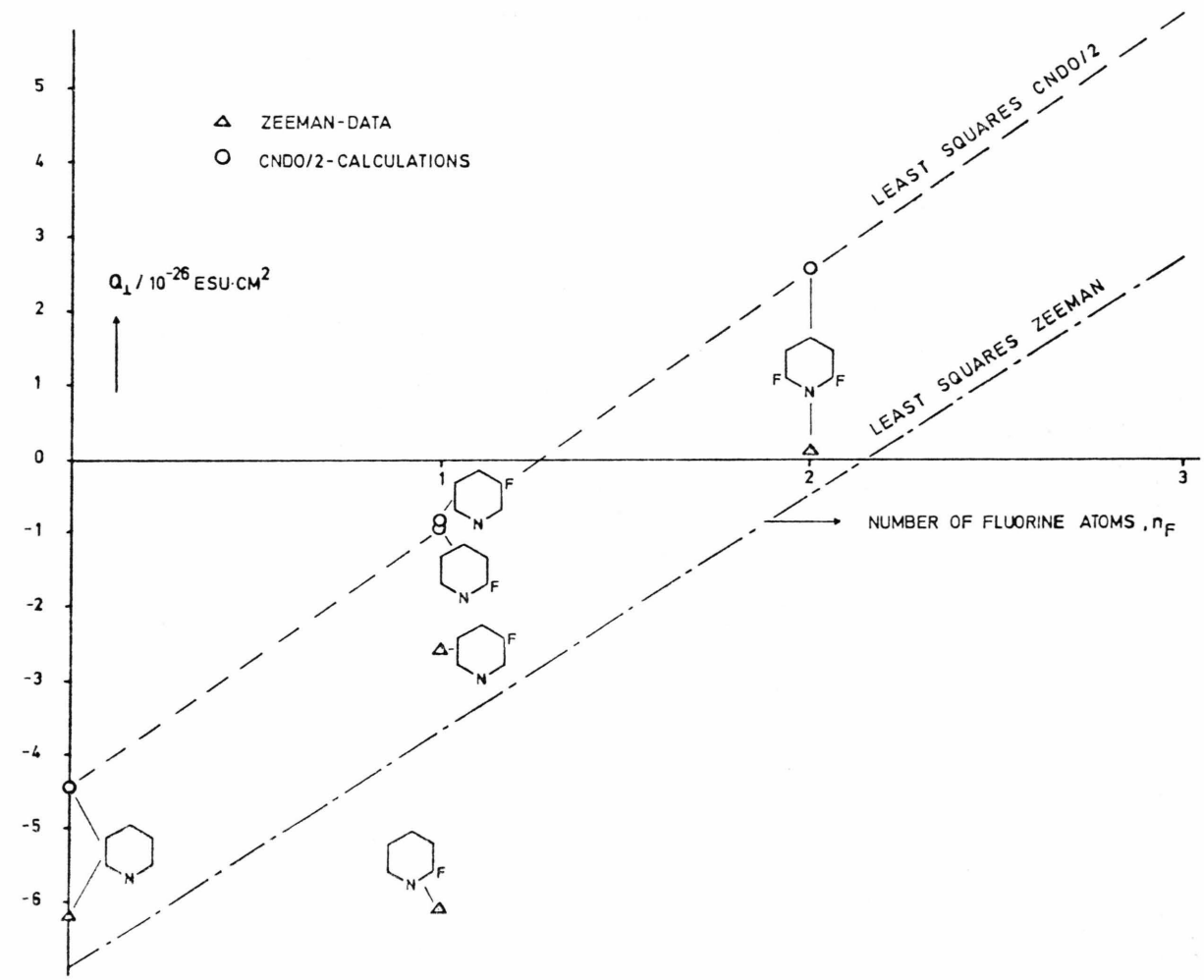

Fig. 6. In this Figure we show plots of the out of plane component of the molecular electric quadrupole moments for the Fluoropyridines studied so far. All quadrupole moments are referred to a coordinate system with its origin at the center of the ring. With experimental uncertainties typically on the order of three units (see Table 4 and Ref. [d] and [e] of Table 6) postulation of a linear relationship between $Q_\perp$ and the number of Fluorine substituents may appear to lack a sound experimental foundation. We note however that the least squares straight lines drawn through the experimental data and drawn through the values calculated within the CNDO/2 approximation [51, 52] closely parallel and that the data obtained for the Fluorobenzenes (see Fig. 7) rend further credit to a linear relationship.

$$Q_{zz} = \frac{|e|}{2}\left(\sum_{\nu}^{\text{nuclei}} Z_\nu(2z_\nu^2 - x_\nu^2 - y_\nu^2) - \left\langle 0\left|\sum_{\varepsilon}^{\text{electrons}}(2z_\varepsilon^2 - x_\varepsilon^2 - y_\varepsilon^2)\right|0\right\rangle\right). \quad (2)$$

Z_ν = atomic number of ν-th nucleus, x_ν, y_ν, z_ν = coordinates of ν-th nucleus, $x_\varepsilon, y_\varepsilon, z_\varepsilon$ = coordinates of ε-th electron.

The Q_{zz}-values referred to the center of the ring are obtained from those experimentally determined, Q_{zz}^{exp}, which are referred to the molecular principal inertia axes system, by the transformation

$$Q_\perp = Q_{zz}^{\text{exp}} + \mu_x^{\text{exp}}\Delta x + \mu_y^{\text{exp}}\Delta y, \quad (3)$$

where Δx and Δy are the coordinates of the center of the ring referred to the principal inertia axes system and where μ_x^{exp} and μ_y^{exp} are the components of the molecular electric dipole moment. The experimental values are calculated from the Zeeman data via [49].

$$Q_{zz}^{\text{exp}} = \frac{h|e|}{16\pi^2 m_p}\left\{\frac{2g_{zz}}{B_z} - \frac{g_{xx}}{B_x} - \frac{g_{yy}}{B_y}\right\} - \frac{2mc^2}{|e|}\{2X_{zz} - X_{xx} - X_{yy}\} \quad (4)$$

with h = Planck's constant, m = electron mass, m_p = proton mass, c = velocity of light, B_x, B_y,

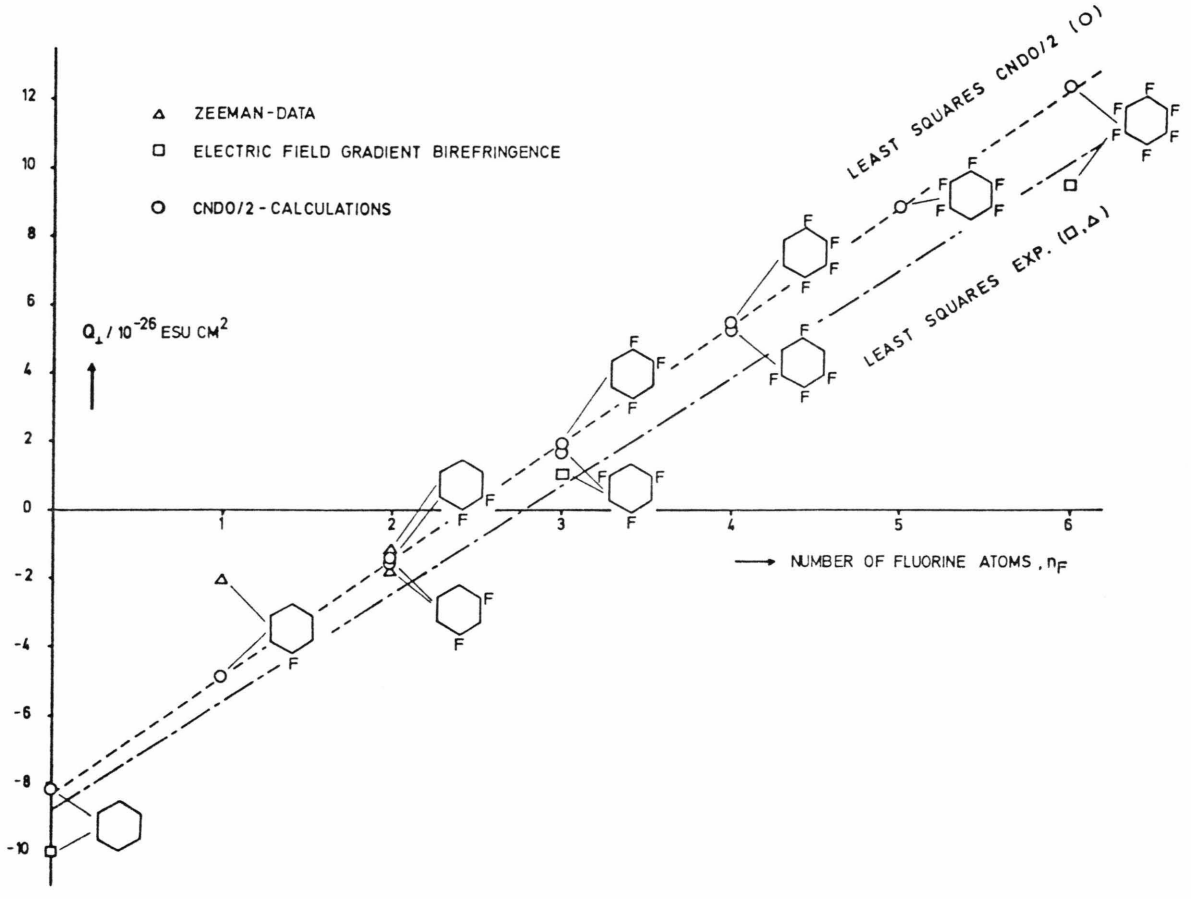

Fig. 7. The out of plane molecular electric quadrupole moments of the Fluorobenzenes obviously closely follow a linear relationship if referred to the center of the Benzene ring and if plotted against the number of Fluorine substituents. Again we also give quadrupole moments calculated from CNDO/2 wave functions as described in [51, 52]. Note that the slopes of the least squares straight lines are essentially identical for the Fluoropyridines (Fig. 6) and the Fluorobenzenes with an increment of approximately 3.2 units per Fluorine substitution.
The experimental values are taken from Ref. [6, 7, 53, 55] and, if necessary, were transformed to the center of the ring according to Eq. (3) of the text.

B_z = rotational constants, g_{xx}, g_{yy}, g_{zz} and X_{xx}, X_{yy}, X_{zz} = diagonal elements of the g- and X-Tensors resp. (The experimental quadrupole moments should come close to the vibrationally averaged ground state expection values as discussed for instance in Ref. [50].)

Note that charge shifts along the perimeter of the ring, leaving $r_n^2 = x_n^2 + y_n^2$ constant, do not change the value of $Q_\perp$.

In Fig. 6 we show such a plot of $Q_\perp$ versus the number of Fluorine substituents for the Fluoropyridines measured so far. Note that the least squares straight line closely parallels the line calculated from the extension of Poples CNDO/2 program described in [51, 52]. In Fig. 7 the corresponding plot is shown for the Fluorobenzenes with experimental data from the rotational Zeeman effect and the electrical field gradient birefringence methods combined. With the slopes in Fig. 6 and 7 practically identical, resulting in an $Q_\perp$-increment of $+3.2 \cdot 10^{-26}$ esu cm^2 for each Fluorine substitution, we think that the Benzene quadrupole moment determined by Vrbancich and Ritchie [53] is essentially correct and that the value proposed earlier by Shoemaker and Flygare [54] on the basis of the rotational Zeeman effect value for Fluorobenzene [55] should be revised.

In this context we would like to state that we think that the theoretical considerations presented by Shoemaker and Flygare are basically correct and that the discrepancy is caused by the experimental uncertainties of the Fluorobenzene data. The $n_F = 0$ intercept of the least squares straight line shown in Fig. 7 is still within the single standard deviation of the Shoemaker/Flygare prediction. To settle this problem we plan to redo the rotational Zeeman effect study of Fluorobenzene with increased precision.

Herrn Professor Helmut Dreizler sei für die kritische Durchsicht des Manuskripts gedankt. — Wir danken der Deutschen Forschungsgemeinschaft und dem Fonds der Chemie für die finanzielle Unterstützung dieser Arbeit. — Die Rechnungen wurden am Rechenzentrum der Universität durchgeführt.

[1] D. H. Sutter and W. H. Flygare, J. Amer. Chem. Soc. **91**, 4063 (1969).
[2] D. H. Sutter and W. H. Flygare, J. Amer. Chem. Soc. **91**, 6895 (1969).
[3] D. H. Sutter, Z. Naturforsch. **26a**, 1644 (1971).
[4] B. Bak, E. Hamer, D. H. Sutter, and H. Dreizler, Z. Naturforsch. **27a**, 705 (1972).
[5] W. Czieslik, D. H. Sutter, H. Dreizler, C. L. Norris, S. L. Rock, and W. H. Flygare, Z. Naturforsch. **27a**, 1691 (1972).
[6] D. H. Sutter, Z. Naturforsch. **29a**, 786 (1974).
[7] W. Czielsik, J. Wiese, and D. H. Sutter, Z. Naturforsch. **31a**, 1210 (1976).
[8] J. Wiese and D. H. Sutter, Naturforsch. **35a**, 712 (1980).
[9] H. C. Longuet-Higgens and L. Salem: Proc. Roy. Soc. London Ser. A **257**, 445 (1960).
[10] F. Sondheimer et al., Chem. Soc. Spec. Publ. No. **21** (1967).
[11] R. C. Haddon, V. R. Haddon, and L. M. Jackman, Top. Curr. Chem. **16**, 103 (1971).
[12] R. C. Haddon, Tetrahedron. **28**, 3613, 3635 (1972).
[13] F. Sondheimer, Acc. Chem. Res. **5**, 81 (1972).
[14] A. G. Anastassion and E. Reichmanis, Angew. Chem. Int. Ed. Engl. **1974**, 404 and references cited therein.
[15] R. B. DuVernet, T. Otsubo, J. A. Lawson, and V. Boekelheide, J. Amer. Chem. Soc. **97**, 1629 (1975).
[16] L. M. Jackman, F. Sondheimer, Y. Amiel, D. A. Ben-Efraim, Y-Gaomi, R. Wolovsky, and A. A. Bothner-By, J. Amer. Chem. Soc. **84**, 4307 (1962).
[17] J. A. Pople and K. G. Untch, J. Amer. Chem. Soc. 88, 4811 (1966).
[18] R. J. Abraham, R. C. Sheppard, W. A. Thomas, and S. Turner, Chem. Commun. **1965**, 43.
[19] J. A. Elvidge, Chem. Commun. **1965**, 160.
[20] T. G. Schmalz, C. L. Norris, and W. H. Flygare, J. Amer. Chem. Soc. **95**, 7961 (1973).
[21] J. R. Davidson, A. K. Burnham, B. Siegel, P. Beak, and W. H. Flygare, J. Amer. Chem. Soc. **96**, 7394 (1971).
[22] A. K. Burnham, Jaekeum Lee, T. G. Schmalz, P. Beak, and W. H. Flygare, J. Amer. Chem. Soc. **99**, 1836 (1976).
[23] W. H. Flygare and R. C. Benson, Mol. Phys. **20**, 225 (1971).
[24] D. H. Sutter and W. H. Flygare, Top. Curr. Chem. **63**, 89 (1976).
[25] H. Mäder, W. Schrepp, and H. Dreizler, Z. Naturforsch. **31a**, 1419 (1976).
[26] H. Mäder, Methoden und Ergebnisse Mikrowellenspektroskopischer Untersuchungen von Rotationsrelaxationen in der Gasphase. Habilitationsschrift, Universität Kiel 1979.
[27] A. Roe and F. Hawkins, J. Amer. Chem. Soc. **69**, 2443 (1947).
[28] G. C. Finger, L. D. Starr, A. Roe, and W. J. Link, J. Org. Chem. **27**, 3965 (1962).
[29] S. D. Sharma and S. Doraiswamy, J. Mol. Spectr. **59**, 216 (1976).
[30] S. Doraiswamy and S. D. Sharma, Chem. Phys. Lett. **37**, 527 (1976).
[31] O. L. Stiefvater, Z. Naturforsch. **30a**, 1765 (1975).
[32] O. L. Stiefvater, Z. Naturforsch. **31a**, 53 (1976).
[33] H. D. Rudolph, Z. Angew. Phys. **13**, 401 (1961).
[34] U. Andresen and H. Dreizler, Z. Angew. Phys. **30**, 207 (1970).
[35] For the nonvaniching matrix elements see for instance: H. P. Benz, A. Bauder, and Hs. H. Günthard, J. Mol. Spec. **21**, 156 (1966).

[36] The least squares procedure is carried out as described for the rotational constants in: L. Engelbrecht and D. H. Sutter, Z. Naturforsch. **31a**, 670 (1976).
[37] D. H. Sutter, Z. Naturforsch. **26a**, 1644 (1971).
[38] K. F. Dössel, J. Wiese, and D. H. Sutter, Z. Naturforsch. **33a**, 21 (1978).
[39] C. M. French, Trans. Faraday Soc. **47**, 1056 (1951).
[40] P. W. Sellwood, Magnetochemistry. Intersci. Publ. New York London 1956.
[41] see Ref. [24], Chapter II C.
[42] J. Wiese, Diplomarbeit Kiel 1975.
[43] J. Wiese and D. H. Sutter, Z. Naturforsch. **35a**, 712 (1980).
[44] F. Rohwer and A. Guarnieri, Z. Naturforsch. **35a**, 336 (1980).
[45] J. A. Pople and D. L. Beveridge, Approximate Molecular Orbital Theory, Mc-Graw-Hill Book Company, New York 1970. The original parameterization was used throughout this work.
[46] This is the basic assumption made by T. G. Schmalz, C. L. Norris, and W. H. Flygare, see Ref. [20]. To account for the subtle differences in local values caused by interactions with neighbouring atoms Hameka (see L. H. Haley and F. Hameka, J. Amer. Chem. Soc. **96**, 2020 (1974) and references cited therein), for the bulk susceptibilities, has introduced a scheme in which the susceptibility is broken up into a sum of contributions from the cores, bonds and lone paires in the molecule. To set up a similar scheme for the individual components of the susceptibility tensor requires considerably increased experimental data input and has not been carried out so far. We believe however that the less sophisticated model of local atom susceptibilities is sufficient to establish trends within a group of closely related molecules such as the Fluorobenzenes and Fluoropyridines.
[47] See Ref. [24], Chapter II a.
[48] M. P. Bogaard, A. D. Buckingham, M. A. Corfield, D. A. Dunmur, and A. H. White, Chem. Phys. Lett. **12**, 558 (1972).
[49] W. Hüttner, M. K. Lo, and W. H. Flygare, J. Chem. Phys. **48**, 1206 (1968).
[50] See Ref. [24], Chapter II b.
[51] E. Hamer, PHD thesis, Kiel 1973.
[52] E. Hamer, L. Engelbrecht, and D. H. Sutter, Z. Naturforsch. **29a**, 924 (1974). Values are calculated according to Eq. (21) when all superscripts are changed to "CNDO/2".
[53] J. Vrbancich and G. L. D. Ritchie, J. Chem. Soc. Faraday II **76**, 648 (1980).
[54] R. L. Shoemaker and W. H. Flygare, J. Chem. Phys. **51**, 2988 (1969).
[55] W. Hüttner and W. H. Flygare, J. Chem. Phys. **50**, 2863 (1969).
[56] E. Hamer and D. H. Sutter, Z. Naturforsch. **31a**, 265 (1976).